PHYSICAL REVIEW C VOLUME 23, NUMBER 1 JANUARY 1981

# Target residue recoil properties in the interaction of 8.0 GeV $^{20}$Ne with $^{181}$Ta

W. Loveland
*Department of Chemistry, Oregon State University, Corvallis, Oregon 97331*

D. J. Morrissey, K. Aleklett,* and G. T. Seaborg
*Nuclear Science Division, Lawrence Berkeley Laboratory, University of California, Berkeley, California 94720*

S. B. Kaufman, E. P. Steinberg, and B. D. Wilkins
*Chemistry Division, Argonne National Laboratory, Argonne, Illinois 60439*

J. B. Cumming, P. E. Haustein, and H. C. Hseuh
*Chemistry Department, Brookhaven National Laboratory, Upton, New York 11973*
(Received 27 May 1980)

The thick target, thick catcher technique has been applied to determine the average kinematic properties of a number of target-fragmentation products formed in the reaction of 8.0 GeV (400 MeV/$A$) $^{20}$Ne with $^{181}$Ta. The forward momentum transferred to the target as a function of product mass is larger than that for the reaction of 25 GeV $^{12}$C or relativistic protons with heavy targets, suggesting that limiting fragmentation has not been achieved in the interaction of 8 GeV $^{20}$Ne projectiles with a $^{181}$Ta target.

[NUCLEAR REACTIONS $^{181}$Ta($^{20}$Ne, spallation), $E = 8.0$ GeV; measured target residue recoil properties; relativistic heavy ion reactions; thick target, thick catcher technique; Ge(Li) spectroscopy.]

## I. INTRODUCTION

The concept of "limiting fragmentation"[1] or "scaling"[2] has been used widely to describe target fragmentation in relativistic nuclear collisions. This hypothesis states that the distribution of products in the rest frame of the projectile or target approaches a limiting form as the bombarding energy increases or, experimentally, that a particular distribution changes negligibly over a large range of bombarding energies. The physical basis of this concept is that, due to Lorentz contraction of the projectile, the projectile-target interaction time at any given impact parameter becomes independent of bombarding energy.

Support for the application of this concept to describe relativistic nuclear collisions comes from the observation of Cumming *et al.*[3] that the product mass and charge distributions from the spallation of Cu by 80 GeV $^{40}$Ar, 25 GeV $^{12}$C, and 3.9 GeV $^{14}$N were similar and the observation of Loveland *et al.*[4] that the same situation occurs in the interactions of 8 GeV $^{20}$Ne and 25 GeV $^{12}$C with $^{181}$Ta. For both Cu and Ta targets the distributions from the relativistic heavy ion reactions were generally similar to the distributions produced in reactions induced by protons of the same total kinetic energy. These observations coupled with the observation of Kaufman *et al.*[5] that the forward momentum transferred to a $^{197}$Au target nucleus by 25 GeV $^{12}$C ions was essentially identical to that transferred by 28 GeV protons suggested that limiting fragmentation might describe the product kinematic properties over a wide range of projectile energies. Small deviations from the limiting fragmentation hypothesis were observed, however, for the recoil properties of fragments from the reaction of 25 GeV $^{12}$C with Cu.[6] It has long been known in the case of proton induced reactions that cross sections become independent of projectile energy at much lower energy than do the product kinematic properties such as the mean forward momentum transfer. We therefore sought to determine the mean product kinematic properties for the reaction of an intermediate energy projectile 8.0 GeV $^{20}$Ne with a heavy target $^{181}$Ta using the thick target, thick catcher technique.

We found that the product kinetic properties are *not* independent of bombarding energy for the (projectile-target) energy and mass region spanned by the 8 GeV $^{20}$Ne + $^{181}$Ta and 25 GeV $^{12}$C + $^{197}$Au reactions and furthermore, that the specific product forward momenta observed in the reaction of 8.0 GeV $^{20}$Ne with $^{181}$Ta exceed those observed in relativistic proton induced reactions with heavy targets. The good agreement between the independent measurements of the three laboratories demonstrates that these important kinematic parameters describing relativistic nuclear collisions can be reliably measured.

## II. EXPERIMENTAL

A stack of $^{181}$Ta metal foils (see Fig. 1) was irradiated for approximately 18 h (total particle fluence $3.6\times10^{13}$ $^{20}$Ne) with an external beam of 8.0 GeV $^{20}$Ne ions at the LBL Bevalac. In this foil stack there were three separate target assemblies belonging to the cooperating groups from LBL, ANL, and BNL. The LBL targets consisted of three $^{181}$Ta foils (of thickness 40.4, 42.5, and 41.6 mg/cm$^2$) surrounded by forward and backward Mylar catcher foils of thickness 35.5 mg/cm$^2$. As shown in Fig. 1, the three LBL targets were spatially separated from each other by a distance of 8 cm. The ANL target stack consisted of four $^{181}$Ta foils (total $^{181}$Ta thickness 176 mg/cm$^2$), each surrounded by two Mylar catcher foils of thickness 18 mg/cm$^2$. Guard foils (18 mg/cm$^2$ Mylar) intervened between each of the four ANL targets and the assembly was vacuum sealed in a Mylar envelope. The BNL target stack consisted of a single $^{181}$Ta foil of thickness 92.6 mg/cm$^2$ surrounded on each side by three 18 mg/cm$^2$ Mylar foils and vacuum sealed in a Mylar envelope. The target assemblies thus represented a variety of approaches to the problem of target arrangement and comparisons between the results of the different groups were expected to be enlightening concerning the role of reactions induced by secondary particles in these studies. The total beam energy loss in the combined target assembly was calculated to be ~230 MeV with a beam attenuation due to nuclear scattering of 4.5%.

Assay of the radioactivities in the LBL targets and catcher foils by x-ray and $\gamma$-ray spectroscopy began approximately two hours after the end of irradiation. The assay of the BNL and ANL target radioactivities began 30 h after the end of irradiation with these measurements being delayed by air shipment of the targets to the respective laboratories. In the case of the LBL targets, the three forward catcher foils were placed together and counted as a single sample as were the three backward foils. One representative $^{181}$Ta foil was counted and a correction for the uncounted targets was made to each nuclide activity. A similar procedure was followed for the ANL targets except that all target foils were placed together and counted as a single high activity sample.

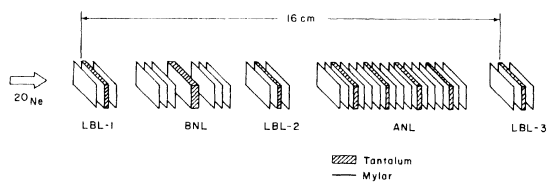


FIG. 1. Schematic diagram of target foil array.

Standard techniques which have been described elsewhere[3,7,8] were used to identify the radionuclides present in each sample and to determine the activity of each nuclide in the forward, backward, and target foils. No corrections were made to any of the foil activities for the effect of secondary induced reactions because previous studies[9] had shown that over the range of target thicknesses encountered in this experiment, the effect of secondary reactions was negligible ($\leq 4\%$) and our own observation that the measurements of the different laboratories using vastly different target arrangements were the same within experimental uncertainty. The guard foils were used to measure the amount of any products whose range exceeded the thickness of the catcher foils, as well as any activity due to impurities. The only such activity found was that of $^{24}$Na from impurity activation; the correction for this effect amounted to $\leq 1\%$.

## III. RESULTS

The results of these measurements are the fractions of each radionuclide which recoiled out of a target of thickness $W$ (mg/cm$^2$) in the forward and backward directions denoted by $F$ and $B$, respectively. Table I gives a tabulation of the individual results of the three groups for the forward-to-backward ratio ($F/B$) and a quantity approximately equal to the mean range of the recoil in the target material, $2W$ ($F+B$). Also shown in Table I and plotted in Fig. 2 are the weighted averages of the measurements of the different laboratories which, in general, agreed within experimental uncertainty. Each product recoil property reported in Table I was measured by at least two of the three laboratories. In calculating the weighted averages, the minimum uncertainty in the results from a single laboratory was arbitrarily assumed to be ±5%, although the reported uncertainty may have been less. This procedure was done to ensure that each laboratory's results affected the average in this comparison and because we believe there are systematic uncertainties in this type of measurement of at least 5%.

The results were transformed into kinematic quantities using the two step vector model of high energy nuclear reactions, developed by Sugarman and co-workers.[10-12] The equations used in the analysis have recently been described by Winsberg.[13] In this model, the velocity $\vec{V}_l$ of a recoil nuclide in the laboratory system is taken to be the sum of the two vectors

$$\vec{V}_l = \vec{v} + \vec{V} .$$

The velocity vector $\vec{v}$ results from the initial fast

TABLE I. Target fragment recoil properties for 8.0 GeV $^{20}$Ne + Ta.

| Nuclide | $E$ (keV) | LBL $F/B$ | LBL $2W$ $(F+B)$ | ANL $F/B$ | ANL $2W(F+B)$ | BNL $F/B$ | BNL $2W$ $(F+B)$ | Wtd average $F/B$ | Wtd average $2W$ $(F+B)$ |
|---|---|---|---|---|---|---|---|---|---|
| $^{24}$Na | 1368.6, 2753.9 | 5.9±0.4 | 17.1 ±1.7 | 5.44±0.30 | 15.8 ±1.0 | 5.90±0.13 | 17.42±0.33 | 5.72±0.19 | 16.77±0.61 |
| $^{28}$Mg | 1777.8 | 5.2±0.8 | 13.7 ±1.4 | 4.71±0.35 | 15±1.6 | 4.64±0.23 | 13.71±0.88 | 4.69±0.19 | 13.9 ±0.68 |
| $^{43}$K | 617.8 | 3.4±0.7 | 9.8 ±2.0 | 3.4 ±0.5 | 7.1 ±1.0 | | | 3.40±0.41 | 7.64±0.89 |
| $^{46}$Sc | 889.3, 1120.5 | | | 3.07±0.2 | 6.9 ±0.8 | 3.09±0.09 | 6.94±0.48 | 3.08±0.12 | 6.93±0.32 |
| $^{48}$Sc | 1037.5, 1312.1 | 3.1±0.6 | 6.2 ±0.9 | 3.11±0.25 | 7.2 ±0.9 | 3.11±0.17 | 7.91±0.26 | 3.11±0.14 | 7.57±0.34 |
| $^{48}$V | 983.5, 1312.1 | | | 3.06±0.25 | 7.4 ±0.5 | 3.02±0.20 | 7.64±0.16 | 3.04±0.16 | 7.55±0.30 |
| $^{54}$Mn | 834.8 | | | 2.97±0.30 | 6.9 ±0.8 | 2.61±0.27 | 7.22±0.34 | 2.77±0.20 | 7.17±0.33 |
| $^{65}$Zn | 1115.5 | | | 2.8 ±0.7 | 5.9 ±0.9 | 2.27±0.39 | 6.49±0.66 | 2.40±0.34 | 6.28±0.53 |
| $^{74}$As | 595.6 | 3.3±0.8 | 4.7 ±0.9 | 2.77±0.25 | 5.7 ±0.6 | 2.54±0.20 | 5.25±0.18 | 2.65±0.15 | 5.28±0.23 |
| $^{75}$Se | 264.6 | | | 3.3 ±0.5 | 4.7 ±0.6 | 2.45±0.29 | 4.68±0.26 | 2.66±0.25 | 4.68±0.24 |
| $^{83}$Rb | 529.5, 552.7 | | | 3.95±0.6 | 4.0 ±0.5 | 3.49±0.36 | 4.79±0.37 | 3.61±0.31 | 4.51±0.30 |
| $^{84}$Rb | 881.5 | | | 3.1 ±0.3 | 5.3 ±0.7 | 2.70±0.30 | 5.42±0.29 | 2.90±0.21 | 5.4 ±0.27 |
| $^{87}$Y | 388.3, 484.8 | 4.7±0.5 | 3.9 ±0.4 | 3.8 ±0.4 | 5.0 ±0.6 | 4.28±0.09 | 4.28±0.07 | 4.27±0.16 | 4.17±0.16 |
| $^{89}$Zr | 909.2 | 2.2±0.2 | 3.1 ±0.5 | 4.2 ±0.4 | 4.3 ±0.4 | 4.58±0.12 | 4.40±0.08 | 4.50±0.20 | 4.38±0.19 |
| $^{90}$Nb | 1129.2 | 4.3±0.9 | 3.6 ±0.7 | 4.9 ±0.6 | 4.3 ±0.5 | 6.3 ±1.3 | 3.94±0.34 | 4.92±0.47 | 3.99±0.26 |
| $^{96}$Tc | 778.2, 849.9 | 3.6±1.1 | 4.3 ±0.9 | 4.8 ±0.7 | 4.1 ±0.8 | 4.96±0.43 | 4.31±0.17 | 4.78±0.35 | 4.30±0.21 |
| $^{97}$Ru | 215.7 | 5.0±1.5 | 4.7 ±0.5 | 7.8 ±0.8 | 3.0 ±0.6 | | | 7.18±0.71 | 4.00±0.38 |
| $^{131}$Ba | 496.2 | | 2.5 ±0.4 | 16±3 | 2.0 ±0.25 | 13.5 ±1.0 | 2.30±0.03 | 13.75±0.95 | 2.26±0.10 |
| $^{139}$Ce | 165.8 | | | 15±4 | 1.9 ±0.2 | 17.8 ±6.4 | 1.95±0.04 | 15.79±3.39 | 1.94±0.09 |
| $^{145}$Eu | 893.7 | | 1.4 ±0.2 | 20±3 | 1.35±0.12 | 16.9 ±3.5 | 1.59±0.06 | 18.69±2.28 | 1.50±0.06 |
| $^{146}$Gd | 115.5, 747.1 | | | 19±3 | 1.37±0.20 | 13.3 ±2.5 | 1.58±0.03 | 15.64±1.92 | 1.55±0.07 |
| $^{149}$Gd | 149.7 | 25±15 | 1.0 ±0.1 | 23±4 | 1.31±0.15 | 16.5 ±1.9 | 1.36±0.02 | 17.70±1.72 | 1.26±0.05 |
| $^{167}$Tm | 207.8 | | 0.2 ±0.05 | 11±3 | 0.39±0.06 | 11.3 ±2.1 | 0.42±0.03 | 11.20±1.72 | 0.37±0.02 |
| $^{171}$Lu | 739.6 | | 0.08±0.04 | 8.6 ±2.5 | 0.22±0.04 | 10.0 ±1.7 | 0.23±0.01 | 9.56±1.41 | 0.22±0.01 |

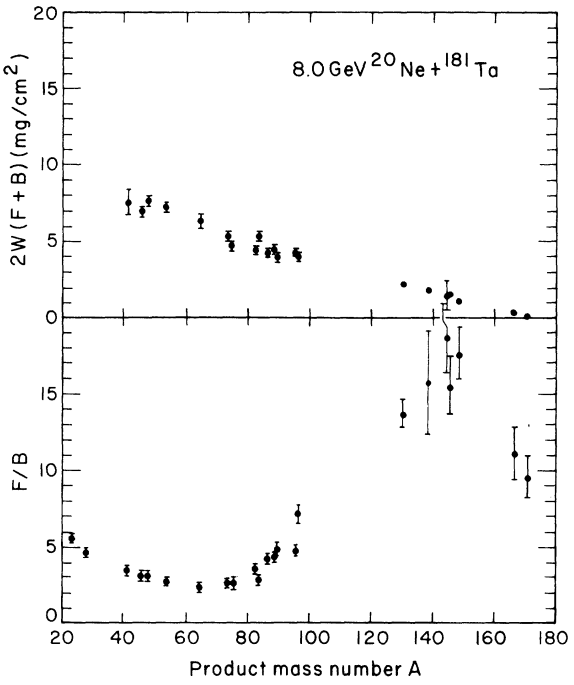


FIG. 2. Target fragment recoil properties from the interaction of 8 GeV $^{20}$Ne with $^{181}$Ta.

projectile-target interaction (the abrasion step of the abrasion-ablation model[14]) while the velocity vector $\vec{V}$, assumed to be isotropic in the moving system, results from the slow deexcitation of the excited primary fragment (the ablation step). The vector $\vec{v}$ is assumed to be constant while the values of the vector $\vec{V}$ are assumed to have a Maxwellian distribution. No correlation is assumed to exist between the two vectors. The vector $\vec{v}$ can be decomposed into its two orthogonal components parallel and perpendicular to the beam ($v_{\parallel}$ and $v_{\perp}$) and in this analysis we have assumed $v_{\perp}=0$. In converting product ranges into kinetic energies, we used the range-energy tables of Northcliffe and Schilling.[15] For ranges lower than those tabulated (as was the case for $^{171}$Lu) a range-proportional-to-energy extrapolation was used. The resulting range-energy curve is in reasonable agreement (±10%) with that predicted by the stopping power theory of Lindhard, Scharff, and Schiott.[16] The results of this analysis are shown in Table II and Fig. 3.

The validity of this analysis depends on the assumptions stated above. The assumption of the isotropy of $\vec{V}$ in the moving system implies that the observed forward peaking seen in the values

TABLE II. Target fragment kinematic properties as deduced from the two step vector model.

| Nuclide | $k$ [a] | $N$ [a] | $R$ (mg/cm$^2$) | $v_{\parallel}$ (MeV/$A$)$^{1/2}$ | $\beta_{\parallel}(=v_{\parallel}/c)$ | $V$ (MeV/$A$)$^{1/2}$ | $\langle E\rangle$ (MeV) |
|---|---|---|---|---|---|---|---|
| $^{24}$Na | 0.543 | 1.71 | 13.9 | 0.651 | 0.021 3 | 1.80 | 44.2 |
| $^{28}$Mg | 0.564 | 1.66 | 11.9 | 0.516 | 0.016 9 | 1.64 | 42.5 |
| $^{43}$K | 1.135 | 1.15 | 6.87 | 0.300 | 0.009 82 | 1.02 | 25.4 |
| $^{46}$Sc | 1.173 | 1.10 | 6.34 | 0.262 | 0.008 60 | 0.960 | 24.0 |
| $^{48}$Sc | 1.195 | 1.10 | 6.90 | 0.275 | 0.009 00 | 0.998 | 27.0 |
| $^{48}$V | 1.129 | 1.09 | 6.90 | 0.290 | 0.009 50 | 1.068 | 31.0 |
| $^{54}$Mn | 1.140 | 1.08 | 6.65 | 0.243 | 0.007 98 | 0.979 | 29.3 |
| $^{65}$Zn | 1.086 | 1.08 | 5.95 | 0.181 | 0.005 92 | 0.842 | 26.1 |
| $^{74}$As | 0.957 | 1.15 | 4.92 | 0.160 | 0.005 24 | 0.676 | 19.1 |
| $^{75}$Se | 0.866 | 1.20 | 4.36 | 0.145 | 0.004 75 | 0.620 | 16.3 |
| $^{83}$Rb | 0.866 | 1.19 | 4.01 | 0.170 | 0.005 57 | 0.555 | 14.5 |
| $^{84}$Rb | 0.871 | 1.19 | 4.97 | 0.168 | 0.005 50 | 0.656 | 20.6 |
| $^{87}$Y | 0.724 | 1.30 | 3.60 | 0.172 | 0.005 63 | 0.510 | 12.8 |
| $^{89}$Zr | 0.711 | 1.311 | 3.76 | 0.149 | 0.004 89 | 0.524 | 13.9 |
| $^{90}$Nb | 0.691 | 1.31 | 3.33 | 0.180 | 0.005 90 | 0.486 | 12.0 |
| $^{96}$Tc | 0.666 | 1.33 | 3.60 | 0.183 | 0.006 00 | 0.503 | 13.7 |
| $^{97}$Ru | 0.613 | 1.38 | 3.05 | 0.204 | 0.006 67 | 0.448 | 11.0 |
| $^{131}$Ba | 0.322 | 1.76 | 1.44 | 0.154 | 0.005 05 | 0.276 | 5.64 |
| $^{139}$Ce | 0.284 | 1.86 | 1.19 | 0.142 | 0.004 66 | 0.245 | 4.74 |
| $^{145}$Eu | 0.235 | 1.95 | 0.871 | 0.131 | 0.004 30 | 0.217 | 3.87 |
| $^{146}$Gd | 0.228 | 1.96 | 0.947 | 0.130 | 0.004 25 | 0.229 | 4.31 |
| $^{149}$Gd | 0.228 | 1.96 | 0.649 | 0.111 | 0.003 62 | 0.187 | 2.94 |
| $^{167}$Tm | 0.227 | 1.97 | 0.248 | 0.054 | 0.001 77 | 0.108 | 1.10 |
| $^{171}$Lu | 0.197 | 2.00 | 0.153 | 0.0422 | 0.001 38 | 0.090 | 0.78 |

[a] The range of the fragments, $R$, in the target material Ta is assumed to be given as $R = kE^{N/2}$, where $E$ is the kinetic energy of the fragment in the system moving with velocity $v_{\parallel}$.

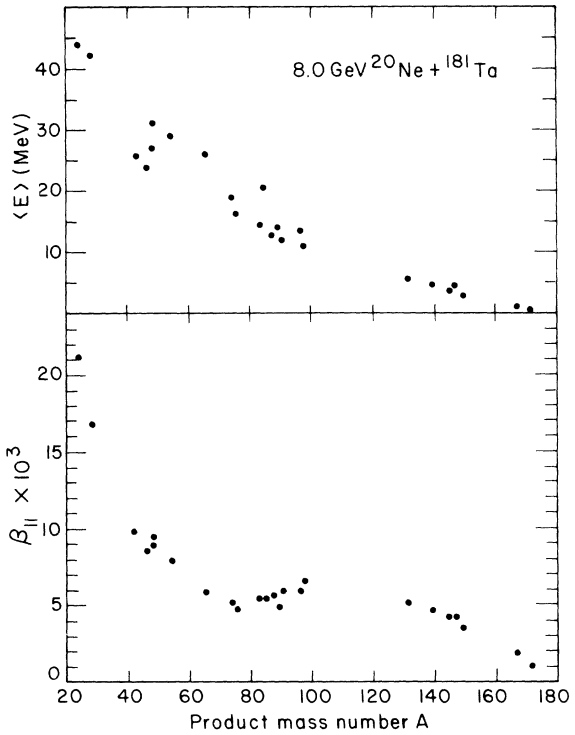


FIG. 3. Target fragment kinetic properties deduced from recoil data using the two-step vector model for the reaction of 8.0 GeV $^{20}$Ne with $^{181}$Ta.

of $F/B$ arises from the forward component of $\vec{v}$, namely $\vec{v}_{\parallel}$. Anisotropies of $\vec{V}$ have been observed[17] for light nuclear fragments in proton-induced reactions at GeV energies, and there may be even larger anisotropies present in relativistic heavy-ion reactions. The investigation of these effects requires measurements of the differential cross sections $d^2\sigma/d\Omega dE$ which have not yet been made, owing to the low beam intensities available. In spite of these uncertainties, however, comparisons between different projectiles and energies can be informative and can guide the course of future investigations.

## IV. DISCUSSION OF RESULTS

Some general features of the data are immediately apparent from Fig. 2. The $F/B$ values represent the extent of forward-peaking of the recoils and thus are a combined measure of the recoil angular distribution and the recoil ranges. As seen in Fig. 2, there is a rapid increase in forward peaking with increasing mass loss from the target (decreasing $A$) until about 40 nucleons have been lost. With further mass loss the $F/B$ values decrease until one reaches the lightest products ($A < 50$) whereupon the $F/B$ values increase with decreasing fragment $A$.

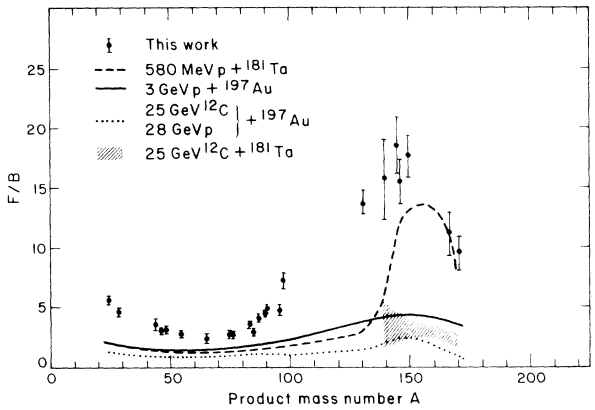


FIG. 4. Comparison of target fragment $F/B$ ratios for various relativistic proton and heavy ion reactions with $^{181}$Ta and $^{197}$Au.

Values of $F/B$ from the present work are compared with results for the interaction of some other energetic projectiles with Ta (Refs. 4, 11, 18, and 19) or Au (Refs. 5 and 8) in Fig. 4. Data from Kaufman *et al.*[8] for protons incident on Au show that the product $F/B$ values are still dependent on projectile energy between 3 and 28 GeV. At higher energies (up to 300 GeV), they are essentially independent of energy. Limited results for the 19 GeV proton irradiation of Ta (Refs. 18 and 19) (not shown in Fig. 4) fall between the 3 and 28 GeV data for Au. Product $F/B$ values for 25 GeV $^{12}$C ions incident on Au (Ref. 5) and Ta (Ref. 4) are generally similar to those observed in reactions induced by relativistic protons. There does not appear to be a very strong dependence of recoil properties on either projectile type or on changes from Ta to Au targets at these high energies. The present results for the reaction of 8.0 GeV $^{20}$Ne ions with Ta are significantly different over the entire mass range from any of the above in that the $F/B$ values are larger, particularly for products with $A > 100$. They are even greater than those observed[18,19] for protons of nearly the same velocity (580 MeV compared with 400 MeV) except for the heaviest products ($A \sim 170$). From this we can conclude that limiting fragmentation has not been attained in the interaction of 8 GeV $^{20}$Ne with $^{181}$Ta. This idea is further supported by the failure[9] of the abrasion-ablation model to describe the product mass and charge distributions in the reaction of 8.0 GeV $^{20}$Ne with $^{181}$Ta. This model, which is based upon the assumption of limiting fragmentation, has been successfully applied[20] to describe the product mass and charge distributions in the reaction of 25.2 GeV $^{12}$C ions with a wide range of nuclei. This inapplicability of limiting fragmentation (with respect to kinetic properties) appears to be nomin-

ally at variance with the work of Cumming *et al.*[3] who found the product mass yield curves to be very similar for the interaction of 3.9 GeV $^{14}$N and 25.2 GeV $^{12}$C with copper (e.g., limiting fragmentation with respect to product yields). We feel that we can understand this difference in terms of the fact that the mass yield curves are not sensitive indicators of some details of the reaction mechanism (see discussion below). This raises the question of when the onset of limiting fragmentation takes place. A reasonable criterion might be that this might occur when the projectile velocity $V_p$ is $0.9c$, i.e., 20 GeV $^{20}$Ne, based upon the idea that further increases in the projectile velocity could only change the interaction time by 10%. At 8.0 GeV $^{20}$Ne, $V_p = 0.71c$ and limiting fragmentation might not be expected.

The insensitivity of product mass yield curves to some important details of the reaction mechanism as indicated by the comparison of the results of this work and those by Cumming *et al.* is given further confirmation by examining the results of Loveland *et al.*[4] who found with the exception of products with $A < 50$, the product mass distributions, from the reaction of 25.2 GeV $^{12}$C, 8.0 GeV $^{20}$Ne, and 5.7 GeV $p$ with $^{181}$Ta were very similar (see Fig. 5). This insensitivity of the product mass distributions to details of the reaction mechanism can be understood in terms of the calculations of Morrissey *et al.*[21] who showed that for $^{40}$Ar projectile (or target) fragments that were more than ~1 charge unit away from the projectile (target), the product mass and charge distributions were not sensitive to the primary product distribution after the fast step of the reaction but rather were governed by the shape of the valley of $\beta$ stability and other parameters related to the statistical deexcitation of the products.

It is instructive to compare the momenta imparted to selected target fragments in the ablation phase (or second step) of the reaction since variation of this property with changes of projectile type and energy can reveal the extent to which the ablation phase of the reaction mechanism is influenced by the abrasion process which occurs during the initial projectile-target interaction. Figure 6 shows a plot of $\langle P \rangle = A\langle V \rangle$ versus $A$ for the spallation of Ta by 8.0 GeV $^{20}$Ne and by protons of 0.45,[11] 0.58,[18,19] and 19 GeV.[18,19]

For the 8.0 GeV $^{20}$Ne induced reaction a steady increase in $\langle P \rangle$ is observed as one moves from near-target products to those that have resulted from the removal of ~50 nucleons from $^{181}$Ta. This increase in $\langle P \rangle$ goes approximately as $\sqrt{\Delta A}$, and is indicative of sequential, stepwise momentum "kicks" being imparted, in a random walk fashion, to the ablating target fragment. A semiempirical theory for such processes developed for proton induced reactions[22] predicts that $\langle P \rangle$ should vary from 15.2 (MeV $A$)$^{1/2}$ for $^{171}$Lu to 34.5 (MeV $A$)$^{1/2}$ for $^{131}$Ba in agreement with the trend of the present results. Neidhart and Bächmann[18] have reported no energy dependence of $\langle P \rangle$ for rare earth nuclides formed by irradiation of Ta with 0.58 and 19 GeV protons. Their mean values shown in Fig. 6 fall somewhat below ours for products with $A < 165$ but agree for $^{167}$Tm and $^{171}$Lu. The general pattern based on these results for Ta and those for Au targets[5,8] is that the ablation phase of reactions leading to products with $\Delta A \lesssim 50$ is essentially energy and projectile invariant.

Below $A = 100$ the target fragments from the 8.0 GeV $^{20}$Ne induced spallation of Ta exhibit a satura-

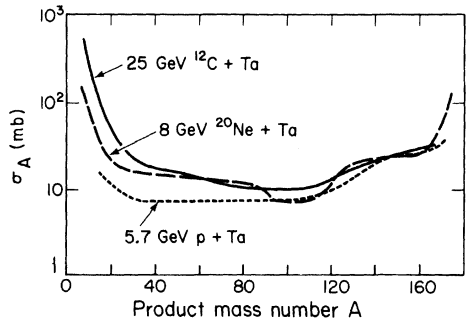


FIG. 5. Target fragment mass distributions for the interaction of 5.7 GeV protons, 8.0 GeV $^{20}$Ne, and 25 GeV $^{12}$C with Ta.

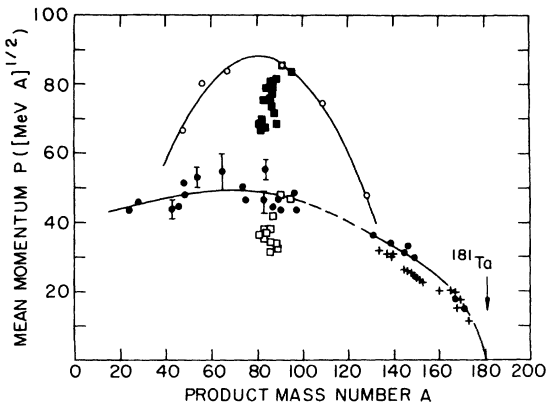


FIG. 6. Dependence of fragment momentum on product mass for the interaction of $^{20}$Ne ions and protons with Ta. Data points are for 8 GeV $^{20}$Ne, •, the present work; 0.45 GeV $^{1}$H, ○, Ref. 11; 0.58 GeV $^{1}$H, ■, Ref. 19; and 19 GeV $^{1}$H, □, also Ref. 19; and the average of 0.58 and 19 GeV $^{1}$H, +, Ref. 18. The solid curve through the filled circles for $A > 130$ is given by $P = 5.15\sqrt{\Delta A}$, where $\Delta A = 181 - A$. The uppermost curve is a parabola through the open circles. The remaining curves serve to guide the eye through the present data.

tion in $\langle P \rangle$ at ~50 (MeV $A$)$^{1/2}$. For comparison with the present results, values of $\langle P \rangle$ obtained by Porile and Sugarman[11] for neutron-rich products such as $^{91}$Sr from the interaction of 0.45 GeV protons with Ta have been included in Fig. 6. These exhibit a parabolic dependence of $\langle P \rangle$ on $A$ centered at $A \approx 81$, consistent with a binary fission mechanism. In a narrow mass region near the peak of the parabola, Trabitzsch and Bächman[19] have studied products with $81 \leq A \leq 95$ spanning a wide range of neutron to proton ratios for 0.58 and 19 GeV protons. Their values of $\langle P \rangle$ shown in Fig. 6 appear to scatter over a considerable range at either energy. As was pointed out by those authors and can be seen in Fig. 7, this reflects a significant dependence of $\langle P \rangle$ on $N/A$. The momenta of products with $74 \leq A \leq 97$ measured in the present experiment fall between but closer to the higher energy proton values. Based on the more extensive data for Au targets,[8] the Ne + Ta values approximate those expected if projectile kinetic energy were the important scaling variable. They are obviously different from those of protons having the same velocity as the $^{20}$Ne. The low values of $\langle P \rangle$ for both $^{20}$Ne ions and 19 GeV protons and the shape of the mass yield curves (Fig. 5) suggest that fission is not a dominant contributor to middle mass products in either case.

In summary of the experimental data, we can say that we have found that in the reaction of 8.0 GeV $^{20}$Ne with $^{181}$Ta, a greater fraction of the products recoil forward than in the reaction of equivalent total energy protons or 25 GeV $^{12}$C ions with heavy targets, but the deexcitation of the fragments following the initial fast step of the reaction proceeds in a similar manner with modest differences between projectile-target systems. The greater $F/B$ ratios in the 8.0 GeV $^{20}$Ne + $^{181}$Ta reaction compared to those observed in the reaction of 25 GeV $^{12}$C with either $^{181}$Ta or $^{197}$Au may be akin to the observed decrease in $F/B$ in proton-induced reactions as the proton energy varies from 3 to 11.5 GeV. For proton induced reactions, this decrease is generally associated[23-26] with a shift in the product angular distribution from forward peaking to sideward peaking. While the mechanism for the sidewise peaking is not established (although interesting arguments concerning nuclear shock waves,[24,27] low energy transverse hadron fluxes,[23] and a fast two body breakup mechanism[28] have been advanced), it may be that studies of relativistic heavy ion reactions will furnish important insights into the details of the mechanism(s) involved. It thus appears that significant opportunities for studying new and exciting aspects of nuclear interactions exist in the study of target fragmentation in relativistic heavy ion reactions and furthermore, that the study of the product angular distributions and momenta hold the greater promise for increasing our understanding of these processes.

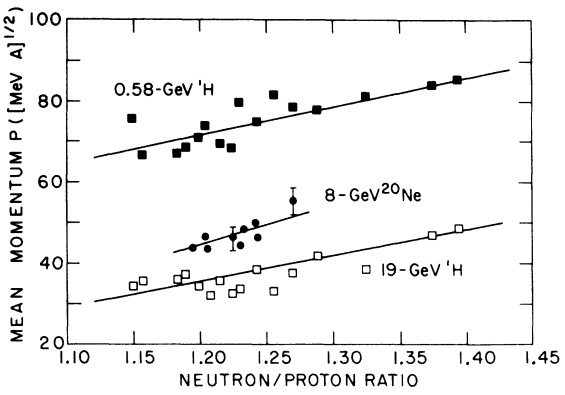


FIG. 7. Dependence of fragment momentum on product neutron/proton ratio. Data are from the present work for $74 \leq A \leq 97$ (●) and Ref. 19 for $81 \leq A \leq 95$ (□ and ■). The lines indicate general trends.

Financial support for this work was provided in part by the U. S. Department of Energy.

*Permanent address: Studsvik Scientific Research Laboratory, Nykoping, Sweden.

[1]J. Benecke, T. T. Chou, C. N. Yang, and E. Yen, Phys. Rev. 188, 2159 (1969).

[2]R. P. Feynman, Phys. Rev. Lett. 23, 1415 (1969).

[3]J. B. Cumming, R. W. Stoenner, and P. E. Haustein, Phys. Rev. C 14, 1554 (1976); J. B. Cumming, P. E. Haustein, R. W. Stoenner, L. Mausner, and R. A. Naumann, *ibid.* 10, 739 (1974); J. B. Cumming, P. E. Haustein, T. J. Ruth, and G. J. Virtes, *ibid.* 17, 1632 (1978).

[4]W. Loveland, D. J. Morrissey, and G. T. Seaborg, Oregon State University Report No. RLO-2227-TA35-1; D. J. Morrissey, W. Loveland, and G. T. Seaborg, Z. Phys. A 289, 123 (1978).

[5]S. B. Kaufman, E. P. Steinberg, and B. D. Wilkins, Phys. Rev. Lett. 41, 1359 (1978).

[6]J. B. Cumming, P. E. Haustein, and H. C. Hseuh, Phys. Rev. C 18, 1372 (1978).

[7]D. J. Morrissey, D. Lee, R. J. Otto, and G. T. Seaborg, Nucl. Instrum. Methods 158, 499 (1978).

[8]S. B. Kaufman, E. P. Steinberg, and M. W. Weisfield, Phys. Rev. C 18, 1349 (1978).

[9]D. J. Morrissey, W. Loveland, M. De Saint-Simon, and G. T. Seaborg, Phys. Rev. C 21, 1783 (1980).

[10]N. Sugarman, M. Campos, and K. Wielgoz, Phys.

Rev. 101, 388 (1956).
[11]N. T. Porile and N. Sugarman, Phys. Rev. 107, 1410 (1957).
[12]N. Sugarman, H. Munzel, J. A. Panontin, K. Wielgoz, M. V. Ramaniah, G. Lange, and E. Lopez-Menchero, Phys. Rev. 143, 952 (1966).
[13]L. Winsberg, Nucl. Instrum. Methods 150, 465 (1978).
[14]J. D. Bowman, W. J. Swiatecki, and C. F. Tsang, Lawrence Berkeley Laboratory Report No. LBL-2908, 1973 (unpublished); see also J. Gossett, H. H. Gutbrod, W. G. Meyer, A. M. Poskanzer, A. Sandoval, R. Stock, and G. D. Westfall, Phys. Rev. C 16, 629 (1977).
[15]L. C. Northcliffe and R. F. Schilling, Nucl. Data A7, 233 (1970).
[16]J. Lindhard, M. Scharff, and H. E. Schiott, K. Dan. Vidensk. Selsk., Mat. Fys. Medd. 33, 14 (1963).
[17]J. B. Cumming, R. J. Cross, J. Hudis, and A. M. Poskanzer, Phys. Rev. 134, B167 (1964); A. M. Poskanzer, G. Butler, and E. K. Hyde, Phys. Rev. C 3, 882 (1971); G. D. Westfall, R. Sextro, A. M. Poskanzer, A. Zebelman, G. Butler, and E. K. Hyde, *ibid.* 17, 1368 (1978).
[18]B. Neidhart and K. Bachmann, J. Inorg. Nucl. Chem. 34, 423 (1972).
[19]U. Trabitzsch and K. Bachmann, Radiochim. Acta 16, 129 (1974).
[20]D. J. Morrissey, W. R. Marsh, R. J. Otto, W. Loveland, and G. T. Seaborg, Phys. Rev. C 18, 1267 (1978).
[21]D. J. Morrissey, L. F. Oliveira, J. O. Rasmussen, G. T. Seaborg, Y. Yariv, and Z. Fraenkel, Phys. Rev. Lett. 43, 1179 (1979).
[22]V. P. Crespo, J. B. Cumming, and J. M. Alexander, Phys. Rev. C 2, 1777 (1970).
[23]D. R. Fortney and N. T. Porile, Phys. Lett. 76B, 553 (1978).
[24]L. P. Remsberg and D. G. Perry, Phys. Rev. Lett. 35, 361 (1975).
[25]N. T. Porile, S. Pandian, H. Klonk, C. R. Rudy, and E. P. Steinberg, Phys. Rev. C 19, 1832 (1979).
[26]N. T. Porile, D. R. Fortney, S. Pandian, R. A. Johns, T. Kaiser, K. Wielgoz, T. S. K. Chang, N. Sugarman, J. A. Urbon, D. J. Henderson, S. B. Kaufman, and E. P. Steinberg, Phys. Rev. Lett. 43, 918 (1979).
[27]A. E. Glassgold, W. Heckrotte, and K. M. Watson, Ann. Phys. (N.Y.) 6, 1 (1959).
[28]B. D. Wilkins, S. B. Kaufman, E. P. Steinberg, J. A. Urbon, and D. J. Henderson, Phys. Rev. Lett. 43, 1080 (1979).